Modelling fomite mediated SARS-CoV-2 exposure through PPE doffing in a hospital environment

Short title: Healthcare worker exposure risk to SARS CoV-2 from PPE behaviours

Marco-Felipe King[1*], Amanda M Wilson[2], Mark H. Weir[3], Martín López-García[4], Jessica Proctor[1], Waseem Hiwar[1], Amirul Khan[1], Louise A. Fletcher[1], P. Andrew Sleigh[1], Ian Clifton[5], Stephanie J. Dancer[6,7], Mark Wilcox[8], Kelly A. Reynolds[2] and Catherine J. Noakes[1]

[1]School of Civil Engineering, University of Leeds, Woodhouse Lane, Leeds, LS2 9JT, UK.

[2]Department of Community, Environment, and Policy, Mel and Enid Zuckerman College of Public Health, University of Arizona, Tucson, AZ, USA

[3]Division of Environmental Health Sciences, The Ohio State University, Columbus, OH, United States of America

[4]School of Mathematics, University of Leeds, Woodhouse Lane, Leeds, LS2 9JT, UK.

[5]Department of Respiratory Medicine, St. James's Hospital, University of Leeds, Leeds, UK

[6] School of Applied Sciences, Edinburgh Napier University, Edinburgh, UK.

[7] Department of Microbiology, Hairmyres Hospital, NHS Lanarkshire, G758RG, UK.

[8]Healthcare Associated Infections Research Group, Leeds Teaching Hospitals NHS Trust and University of Leeds, Leeds, UK

* Corresponding author

Acknowledgements

The authors thank Marc P. Verhougstraete, PhD; Christina Liscynesky, MD for their shared expertise and experience that contributed to the development of the modelled scenarios in this study. This research is funded by the Engineering and Physical Sciences Research Council, UK: Healthcare Environment Control, Optimisation and Infection Risk Assessment (https://HECOIRA.leeds.ac.uk) (EP/P023312/1). M. López-García was funded by the Medical Research Council, UK (MR/N014855/1). J. Proctor was funded by EPSRC Centre for Doctoral Training in Fluid Dynamics at Leeds (EP/L01615X/1). Under a Creative Commons Zero v1.0 Universal license (CC-BY), code can be accessed at: https://github.com/awilson12/surface-contam-model-COVID19

Abstract

Self-contamination during doffing of personal protective equipment (PPE) is a concern for healthcare workers (HCW) following SARS-CoV-2 positive patient care. Staff may subconsciously become contaminated through improper glove removal, so quantifying this exposure is critical for safe working procedures. HCW surface contact sequences on a respiratory ward were modelled using a discrete-time Markov chain for: IV-drip care, blood pressure monitoring and doctors' rounds. Accretion of viral RNA on gloves during care was modelled using a stochastic recurrence relation. In the simulation, the HCW then doffed PPE and contaminated themselves in a fraction of cases based on increasing case load. A parametric study was conducted to analyse the effect of: 1a) increasing patient numbers on the ward, 1b) the proportion of COVID-19 cases, 2) the length of a shift and 3) the probability of touching contaminated PPE. The driving factors for exposure were surface contamination and number of surface contacts. Results simulate generally low viral exposures in most of the scenarios considered including on 100% COVID-19 positive wards although this is where the highest self-inoculated dose is likely to occur with median 0.0305 viruses (95% CI=0-0.6 viruses). Dose correlates highly with surface contamination showing that this can be a determining factor for exposure. The infection risk resulting from exposure is challenging to estimate as it will be influenced by factors such as virus variant and vaccination rates.

Keywords: SARS CoV-2; COVID-19; PPE; surface contact transmission; quantitative microbial risk assessment (QMRA); hospital infection model

Practical Implications

Infection risk from self-contamination during doffing PPE is an important concern in healthcare settings, especially on a COVID-19 ward. Fatigue during high workload shifts may result in increased frequency of mistakes and hence risk of exposure. Length of staff shift and number of COVID-19 patients on a ward correlate positively with the risk to staff through self-contamination after doffing. Cleaning of far-patient surfaces is equally important as cleaning traditional "high-touch surfaces", given that there is an additional risk from bioaerosol deposition outside the patient zone.

Introduction

Severe acute respiratory syndrome coronavirus 2 (SARS-CoV-2) is an enveloped virus which has infected in excess of 200 million people to date and caused more than four million deaths worldwide according to Johns Hopkins University's COVID-19 Dashboard (1). Inanimate objects known as fomites may host pathogens and have the potential to contribute to transmission in healthcare environments. This occurs in viral contamination spread (2–4) including SARS-CoV-2 (5, 6). However, it should be noted that there are uncertainties as to the relationship between molecularly detected virus and infectious virus. In terms of persistence, there appears to be similarity between SARS-CoV-1 and 2 on surfaces, where initial concentrations of $10^{3.7}$ Median Tissue Culture Infectious Dose ($TCID_{50}$)/mL (SARS-CoV-2) and of $10^{3.4}$ $TCID_{50}$/mL (SARS-1) reduced to $10^{0.6}$ $TCID_{50}$/mL (SARS-CoV-2) and $10^{0.7}$ $TCID_{50}$/mL (SARS-1) respectively due to decay of viability of the virus after 72 hours on plastic surfaces (7). Persistence on the scale of days under heavy contamination conditions allows an opportunity for exposure through hand-to-fomite contacts. Although personal protective equipment (PPE) such as gloves, gowns, and masks are worn to protect both patient and healthcare worker (HCW) from exposure, self-contamination during PPE doffing processes (8, 9) poses risks to HCW and enables spread from one patient to another during multiple care episodes. SARS-CoV-2 has been detected on healthcare worker PPE (10) and in the environment of rooms where doffing occurs, demonstrating that errors in doffing could facilitate COVID-19 exposure and transmission.

While SARS-CoV-2 has been detected on PPE and patient surfaces, the relationship between viral RNA concentrations and risk of infection is still

93 unknown(11). Bullard et al. (2020) presents $TCID_{50}$ and cycle threshold values relative
94 to days since symptom onset, but these may not be translatable to concentrations
95 on fomites due to the potential for more SARS-CoV-2 genetic material
96 corresponding to inactivated viruses resulting from incomplete surface disinfection
97 practices (12). Quantitative microbial risk assessments (QMRA) involve the use of
98 mathematical models to estimate doses of a pathogen and subsequent infection
99 risk probabilities. Quantifying infection exposure and risk for any given dose can be
100 used to guide intervention decision-making and have been used in other public
101 health contexts, such as in setting water quality standards (13). These typically rely
102 on experimental doses of a microorganism inoculated into healthy participants or
103 mice models in a known quantity. Whether they develop the infection can then be
104 recorded(13). QMRA modelling and surface contact models have been used to
105 evaluate multiple transmission pathways. The role of care-specific behaviours in
106 environmental microbial spread (14) includes the effect of glove use in bacterial
107 spread from one surface to another (15) and evaluating risk reductions through
108 hand hygiene or surface disinfection interventions (16–18). While a strength of QMRA
109 is relating environmental monitoring data to health outcomes, a common limitation
110 has been a lack of specific human behaviour data such as hand-to-face or hand-
111 to-surface contact sequences that result in dose exposures (18, 19). The use of the
112 QMRA modelling framework incorporating care type surface contact patterns
113 before potential self-contamination via PPE doffing will offer insight into viral
114 exposure per shift.
115 The objective of this study is to relate SARS-CoV-2 concentrations on surfaces to
116 predicted exposure ¡for a single healthcare worker over an 8-hour shift and estimate

117 the effects of doffing mistakes and number of care episodes per shift on inoculated
118 dose per shift.

119 *Methodology*

120 This approach combines human behaviour and fomite-mediated exposure
121 models for 19 hospital scenarios, for which concentrations of SARS-CoV-2 on hands
122 and infection risk for a single shift are estimated for a registered nurse, an auxiliary
123 nurse and a doctor. A control scenario was defined as a single episode of care with
124 a SARS-CoV-2 positive individual with an assumed 80% probability of self-
125 contamination during doffing: a "worst case scenario." Eighteen other scenarios
126 covered 3 likelihoods of self-contamination: 10%, 50%, and 80%, x 2 case load
127 conditions: 7 patients (low) vs. 14 patients (high) x 3 probabilities of any given patient
128 being COVID-19 positive: low (5%), medium(50%), and a 100% COVID-19 positive
129 ward. These rates of self-contamination during doffing were assumed due to
130 uncertainty as to how workload and stress, especially under pandemic conditions,
131 would influence doffing. Exploring probabilities of self-contamination as low as 5%
132 and as high as 80% allows for exploration of optimistic and worse case scenarios.
133 During low case load conditions, it was assumed that the number of care
134 episodes per shift would be less (7) than for high load conditions (14). The assumed
135 number of patient care episodes when PPE is worn per shift for low and high case
136 load scenarios were 7 and 14, respectively, based on a respiratory ward in a
137 university teaching hospital in the UK. The low case load estimate was based on
138 communication with a UK NHS consultant, who tracked the number of gowns used
139 by healthcare workers over a week on a mixed COVID-19 8-bed respiratory ward. All
140 model parameters are described and reported in Table 1. Per scenario, three

141 simulations were run where sequences of hand-surface contacts per care episode

142 were care-specific (IV care, observational care, or doctors' rounds).

143 **Table 1.** Model parameters and their distributions/point values

Parameter	Distribution/Point Value	Reference
Surface contamination (C_{RNA}) (RNA/ swabbed surface area)	For infected patient scenarios Surfaces: Triangular (min=3.3 x 10^3, mid=2.8 x 10^4, max=6.6 x 10^4) Patient: Point estimate: 3.3 x 10^3	(20)
Area of any given surface($A_{surface}$) (cm^2)	Triangular (min=5, max=195, mid=100)	Assumed
Fraction of RNA(*infective*) assumed to be infectious	Uniform (min=0.001, max=0.1)	Assumed
Finger-to-surface transfer efficiency (β) (fraction)	Normal (mean=0.118, sd=0.088) Left- and right-truncated at 0 and 1, respectively	(4)
Surface-to-finger transfer efficiency (λ) (fraction)	Normal (mean=0.123, sd=0.068) Left- and right-truncated at 0 and 1, respectively	(4)
Finger-to-mouth transfer efficiency ($TE_{H®M}$) (fraction)	Normal (mean=0.339, sd=0.1318) Left- and right-truncated at 0 and 1, respectively	(21)
Glove doffing self-contamination transfer efficiency	Uniform (min=3 x 10^{-7}, max=0.1)	(8)
T_{99} on Hands (hours) used for calculating inactivation constants	Uniform (min=1, max=8)	(22, 23)
T_{50} on surfaces (hours) used for calculating inactivation constants	Uniform (min=4.59, max=8.17)	(7)
Hand hygiene efficacy: alcohol gel (log_{10} reduction)	Uniform (min=2, max=4)	(24)
Hand hygiene efficacy: soap and water (log_{10} reduction)	Normal (mean=1.62, sd=0.12) Left-and right-truncated at 0 and 4, respectively	(25)
Fraction of total hand surface area for hand-to-mouth or hand-to-surface contacts ($S_m$and S_h)	For in/out events: Uniform (min=0.10, max=0.17) For patient contacts: Uniform (min=0.04, max=0.25) For other surface contacts: Uniform (min=0.008, max=0.25) For hand-to-face contacts:	(26)

	Uniform (min=0.008, max=0.012)	
Total hand surface area (A_h) (cm^2)	Uniform (min=445, max=535)	(19, 27)
Dose response curve parameter* a	0.36 ± 0.25 0.12, 19.6	(28); This study
Dose response curve parameter* β	5.94 ± 11.4 0.27, 802.1	(28); This study

*Dose response curve parameters are to be used in bootstrapped pairs. Mean ± SD and minimum and maximum are provided to offer context as to the magnitude of these parameters.

Healthcare Worker Surface Contact Behaviour Sequences

Fifty episodes of mock patient care were recorded overtly using videography in a respiratory ward side room at St James' Hospital, Leeds. Mock care was undertaken by doctors and nurses with a volunteer from the research team to represent the patient. While these observations were carried out prior to COVID-19, it is assumed that patient care would be similar for any infected patient, including a COVID-19 patient. Ethical approval for the study was given by the NHS Health Research Authority Research Ethics Committee (London - Queen Square Research Ethics Committee), REF: 19/LO/0301. Sequences of surface contacts were recorded for three specific care types: IV drip insertion and subsequent care (IV, n=17) conducted by registered nurses (RN); blood pressure, temperature and oxygen saturation measurement (Observations, n=20) conducted by auxiliary nurses; and doctors' rounds (Rounds, n=13). Data from care were used to generate representative contact patterns to model possible sequences of surface contacts by HCWs in a single patient room. Discrete Markov chains were used, because HCWs were found to touch surfaces in a non-random manner, insofar that transitional probabilities fit to observed behaviours from moving from one surface category were not all equal. By assigning each surface category a numerical value

from 1 to 5, where *Equipment* = 1, *Patient* = 2, *Hygiene areas* = 3, *Near-bed surfaces* = 4, and *Far-bed surfaces* = 5, HCW sequential contact of surfaces can be modelled in terms of weighted probabilities(14). More information regarding the observation of these behaviours and analysis of sequences of events can be seen in King et al. (2020) (29).

The transition of a HCW between surface contacts is modelled using a discrete-time Markov chain approach (14). Using defined weighted probabilities based on observation of patient care, surface contact by HCW can be simulated based on the property that, given the present state, the future and past surfaces touched are independent. This is termed the Markov property (eq 1):

$$P(X_{n+1} = i | X_n = j) \quad (1)$$

Where X_n represents the surface contacted in the n^{th} event, i and j are two surfaces, and P represents a conditional probability. This is then denoted $P_{j \to i}$ for ease of notation. For example, the probability if the HCW is currently touching the table that they will next touch the chair is $P_{table \to chair}$ and can be worked out by counting the number of times this happens during care divided by the number of times any surface is touched after the table(30).

Discrete-time Markov chains were fitted to observed care contact sequences using the "markovchainFit" function from the R package *markovchain (version 0.7.0)*. Separate Markov chains were fitted to IV care, doctors' rounds and observational care sequences. States included "in" (entrance to the patient room), "out" (exit from the patient room), contact with a far-patient surface, contact with a near-patient surface, contact with a hygiene surface (e.g. tap, sink, soap or alcohol dispenser), and contact with equipment. For each episode of care, the first event

was entrance into the patient room. It was assumed in the simulation that all HCWs wore a gown, gloves, mask and face shield when entering the room in that hand-to-face contacts were not modeled during episodes of care, and hand hygiene moments only occurred after doffing in between care episodes. The episode of care ended when an "out" event occurred.

Exposure Model

Accretion of microorganism on hands from surface contacts has been demonstrated (14) to respond to a recurrence relationship with the concentration on hands after the nth contact, C_n^h, with the concentration on hands, C_{n-1}^h, and on the surface involved, C_{n-1}^s, before the contact. See eq. 2.

$$C_n^h = C_{n-1}^h e^{-k_h \Delta t} - S_h\left(\lambda C_{n-1}^h e^{-k_h \Delta t} - \beta C_{n-1}^s e^{-k_s \Delta t}\right) \quad (2)$$

This is an adaptation of the pathogen accretion model (PAM) from King et al. (2015) (14) and a gradient transfer model by Julian et al. (2009) (31). Here, the concentration on hands for contact *n* is equal to the previous concentration on the hand (C_{n-1}^h) after adjusting for inactivation for the virus on the hand (k_h) and surface k_s, minus the removal from the hand due to hand-to-surface transfer plus the gain to the hand due to surface-to-hand transfer. Δt is the time taken for an episode of patient care and sampled from a uniform distribution of range 2-20minutes(32). Here, λ and β represent hand-to-surface and surface-to-hand transfer efficiencies respectively. The fraction of the total hand surface area (S_h) is used to estimate how much virus is available for transfer given a concentration of number of viral particles/cm^2 on the gloved hand and surface.

Estimating Inactivation on the Hand

Sizun et al. (2000) evaluated the survival of human coronaviruses (HCoV) strains OC43 and 229E on latex glove material after drying. Within six hours, there was a reduction in viral infectivity for HCoV-229E that we assume is equal to 99% (22). For HCV-OC43, a reduction of approximately 99% in viral infectivity occurred within an hour (22). Harbourt et al. measured SARS CoV-2 inactivation on pig skin with virus remaining viable for up to 8 hours at 37°C (33). We therefore used a uniform distribution with a minimum of 1 hour and a maximum of 8 hours to estimate a distribution of k_h inactivation rates.

Estimating Inactivation on Surfaces

The decay of the virus causing COVID-19 has been shown to vary under both humidity and temperature but in contrast with previous findings(7), it appears that surface material may not have as large of an impact on decay rate(34). We therefore use one distribution of inactivation rates regardless of surface type by taking a conservative approach and using an averaged half-life τ estimate for stainless steel and plastic-coated surfaces at 21-23°C(7) at 40% relative humidity; which are 5.63h (95%CI=4.59-6.86h), and 6.81h (95%CI=5.62-8.17h), respectively. We assume a first order decay (eq 3) to estimate inactivation constant k which we use here for brevity instead of k_s and k_h in equation 2.

$$C(t) = C_0 e^{-k\,t} \tag{3}$$

Surface viral concentration C at any given time t then depends uniquely on initial concentrationC_0 . Where the half-life τ, is related to k by: $k_s = \log(2) / \tau$. Since hospital rooms are made up of a combination of stainless steel and plastic surfaces, we have taken the widest confidence interval as bounds when sampling from a uniform

distribution for inactivation rate k_s. Inactivation on gloves is assumed to be minimal for the time-scale of a care episode (2-20minutes)(32).

Fractional Surface Area

For contacts with the door handle during "in" or "out" behaviors, a fractional surface area was randomly sampled from a uniform distribution with a minimum of 0.10 and a maximum of 0.17 for open hand grip hand-to-object contacts (26). For contacts with the patient, a fractional surface area was randomly sampled from a uniform distribution with a minimum of 0.04 and a maximum of 0.25, for front partial finger or full front palm with finger contact configurations (26). For contacts with other surfaces, fractional surface areas were randomly sampled from a uniform distribution with a minimum of 0.008 and a maximum of 0.25, spanning multiple contact and grip types from a single fingertip up to a full palm contact (26).

Transfer Efficiencies

All transfer efficiencies used in this model are unitless fractions ranging from 0 to 1, representing the fraction of viruses available for transfer that transfer from one surface to another upon contact. For contacts with surfaces other than the patient, a truncated normal distribution with a mean of 0.123 and a standard deviation of 0.068 with maximum 1 and minimum 0 was randomly sampled for surface-to-finger(λ) transfer efficiencies based on aggregated averages of influenza, rhinovirus and norovirus(4). For patient contacts, transfer efficiencies were randomly sampled from a normal distribution with a mean of 0.056 and a standard deviation of 0.032, left- and right-truncated at 0 and 1, respectively. The mean and standard deviation were informed by transfer efficiencies for rhinovirus measured for direct skin to skin

contact (35). Transfer efficiencies from fingers to surfaces (β)are assumed to be normally distributed with mean 0.118 and standard deviation 0.088(4).

Surface Concentrations

If the patient was assumed to be infected, surface contamination levels (RNA/ swab surface area) were sampled from a triangular distribution where the minimum and maximum were informed by minimum and maximum contamination levels reported for surfaces in an intensive care unit ward (20). The median of these was used to inform the midpoint of the triangular distribution (20). For patient contacts, the concentration of virus detected on a patient mask was used as a point value (3.3 x 10^3RNA/swab surface area) (20). When a patient was not infected, it was assumed contacts with surfaces and with the patient would not contribute to additional accretion of virus on gloved hands.

Surface areas for relating concentrations of RNA/swabbed surface area reported by Guo et al. (2020) to RNA/cm^2 were not provided. While a typical sampling size is 100 cm^2, it may be as small as 10-25 cm^2 (36–39) and in real-world scenarios, sampling surface areas may be larger or smaller than these depending upon available surface area, ease of access and the contamination magnitude expected. Since the surface areas of these surfaces were not provided, a triangular distribution (min=5, max=195, mid=100) describing the surface area (cm^2) of surfaces sampled was used to estimate RNA/cm^2. Not all detected RNA was assumed to represent infectious viral particles. This is a conservative risk approach when utilizing molecular concentration data in QMRA (40). Therefore, concentrations on surfaces C^S (viable viral particles/cm^2) were estimated by eq 4,

$$C^S = \frac{C_{RNA}}{A_{surface}} \cdot infective \quad (4)$$

where C_{RNA} is the RNA/swabbed surface area, $A_{surface}$ is the surface area (cm^2) of the surface, and $infective$ is the fraction of RNA that relates to infective viral particles (uniform(min=0.001, max=0.1)). This overlaps with a range used by Jones (2020) for COVID-19 modeling. While data from Bullard et al. (2020) exist for relating molecularly detected SARS-CoV-2 to culturable SARS-CoV-2 for patient samples, these ratios do not translate to fomite scenarios where surface disinfection likely results in more molecularly detectable virus that does not translate to infectivity. Therefore, we did not use these data to inform our assumptions about viral infectivity for molecularly detected SARS-CoV-2 on surfaces.

Estimating Exposure Dose

For all scenarios, it was assumed the starting concentration on gloved hands for the first episode of care was equal to 0 viral particles/cm2. If gloves were doffed and a new pair was donned in between care episodes, it was assumed the next episode of care began with a concentration of 0 viral particles/cm2 on the gloved hands. After each care episode, a number was randomly sampled from a uniform distribution with a minimum of 0 and a maximum of 1. If this value was less than or equal to the set probability of self-contamination during doffing, self-contamination occurred, where the fraction of total virus transferred from the outer glove surface to the hands was assumed to be uniformly distributed between 3 x 10-5 % and 10% (8). There was then a 50/50 chance that either hands were washed or sanitized using alcohol gel due to lack of available data describing proportions of hand hygiene attributable to these two methods occurring after care episodes. If they washed their hands, a log10 reduction was randomly sampled from a normal distribution with a mean of 1.62 and a standard deviation of 0.12, (min=0 and max=6) (25). While

these are not coronavirus-specific hand washing efficacies they allow for a conservative estimate. If hand sanitizer was used, a log10 reduction was randomly sampled from a uniform distribution with a minimum of 2 and a maximum of 4 (24).

To estimate a dose, an expected concentration on the hands after doffing and hand hygiene was estimated, followed by an expected transfer to a facial mucosal membrane during a single hand-to-nose contact after each patient care episode (eq. 5).

$$D = C_h \cdot TE_{HM} \cdot S_m \cdot A_h \cdot e^{-k_h \Delta t} \quad (5)$$

There was a 50/50 chance that either the right or left hand was used for this hand-to-face contact, as contact patterns between right and left hands have been shown to lack statistically significant differences (41). Here, the transfer efficiency ($T_{H \rightarrow M}$) of the hand-to-nose contact was randomly sampled from a normal distribution with a mean of 33.90%, and a standard deviation of 13.18% based on a viral surrogate(42). These simulated nose contacts were assumed to be with the mucosal membrane as opposed to other parts of the nose, such as the bridge of the nose, that would not result in a dose. The fractional surface area of contact (S_m) was assumed to equal one fingertip. To estimate this surface area, the minimum and maximum front partial fingertip fractional surface areas were divided by 5 to inform the minimum and maximum values of a uniform distribution (22). The surface area of a hand (A_h) was randomly sampled from a uniform distribution with a minimum of 445 cm^2 and a maximum of 535 cm^2 (19) and is informed by values from the Environmental Protection Agency, USA's Exposure Factors Handbook (27). The expected inactivation of virus during this contact assumed a single second contact, and the final k_h value used in the care episode simulation was used. Δt represents

the time between doffing and touching the mucosa. 10,000 parameter combinations are obtained for each care type scenario in a Monte Carlo framework.

Dose-Response

Due to lack of dose-response curve data for SARS-CoV-2, an exact beta-Poisson dose-response curve (43) was fitted to pooled data for SARS-CoV-1 and HCoV 229E, assuming the infectivity of SARS-CoV-2 lies between the infectivity for these two organisms. In eq 6., ${}_1F_1(\alpha, \alpha+\beta, -d)$ is the "Kummer confluent hypergeometric function" and $P(d)$ is the probability of infection risk given dose: d ~~(eq. 6)~~ (43).

$$P(d) = 1 - {}_1F_1(\alpha, \alpha+\beta, -d) \qquad (6)$$

Ten-thousand bootstrapped pairs of α and β were produced based on a maximum likelihood estimation fit. For each estimated dose, an α and β pair were randomly sampled, and an infection risk was estimated with eq. 6. The infectious dose for 50% of infections to occur was between 5 and 100 infectious viral particles with a mean of 30; the dose-response curve can be seen in Figure 1. We use this dose-response curve within the discussion section as a comparator against the curve for HCoV229E also given in (43), which is considered a similar but more infectious virus.

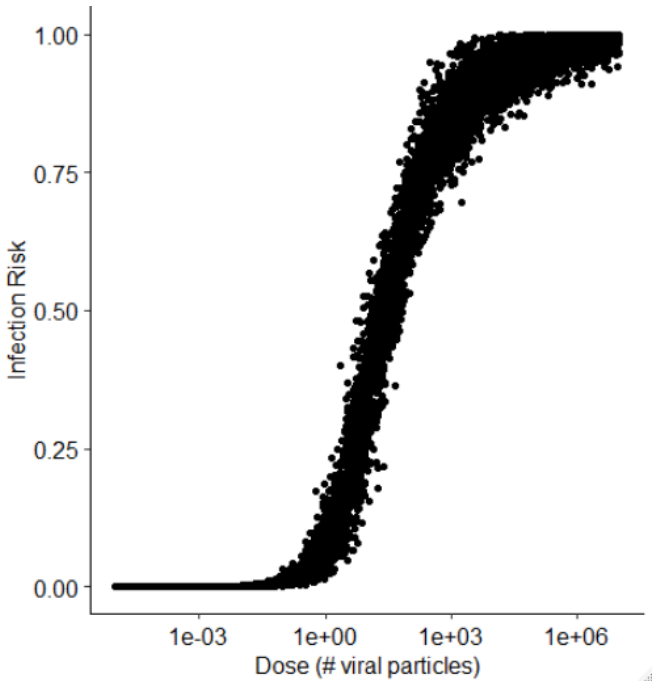

Figure 1 Dose-response risk curve for averaged SARS CoV-1 and Coronavirus 229E response.

Sensitivity Analysis

Spearman correlation coefficients were used to quantify monotonic relationships between input variables and viral exposure. This method has been used in other QMRA studies to evaluate the relationship between model inputs and outputs (31, 44, 45).

Results

Surface contact pattern predictions varied by care type. IV care resulted in the highest number of surface contacts (mean=23, sd=10) per episode, whilst observational care and doctors' rounds had on average 14 (sd=7) and 20 (sd=6) contacts, respectively. A stair plot showing an example HCW surface contact pattern derived from the Markov chain prediction can be seen in **Error! Reference source not found.**.

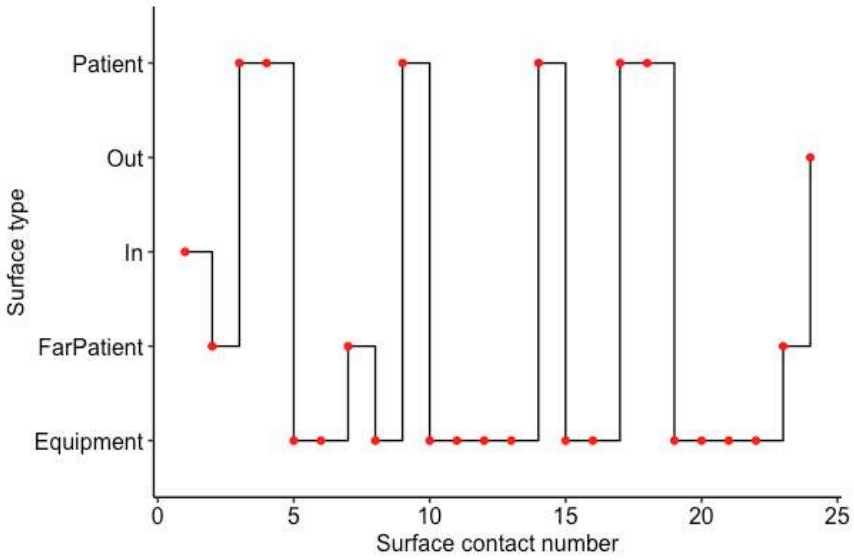

Figure 2 Stair plot of example HCW surface contacts during care, where "patient" is a hand-to-patient contact; "out" and "in" are exit and entrance into the patient room, respectively; "FarPatient" is a hand-to-far patient surface contact; and "Equipment" is a hand-to-equipment surface contact.

Estimated Dose

Dose values in Table 2 and Figure 3 are given in number of virus plaque forming units (PFU), where we also include all fractional values since these would correspond to multiple viruses for a higher surface load relating to different SARS CoV2 variants.

Table 2 PFU doses to for each care type

QUANTILE	IV CARE	OBSERVATIONS	DRS' ROUNDS
0%	0	0	0
25%	0	0	0
50%	0.00184	0.0021	0.00127
75%	0.0751	0.0651	0.0409
95%	0.506	0.421	0.234

Median PFU values for each care type were within the same order of magnitude (see Table 2), whilst maximum values for IV drip were 47% higher than for

observations and 68% than for Drs' rounds which can be explained by the number of surface contacts (IV-drip care: 23±10, Doctors' rounds: 14±7 and Observational care: 20±6). Doubling patient load, regardless of COVID-19 prevalence, probability of self inoculation or care type, caused median viral dose to increase by an order of magnitude from 0.0004PFUs to 0.0069PFUs (95%CI= 0 to 0.501PFU). Figure 3 shows a bar chart with standard deviations for care type, COVID-19 prevalence on the ward and chance of self-contamination.

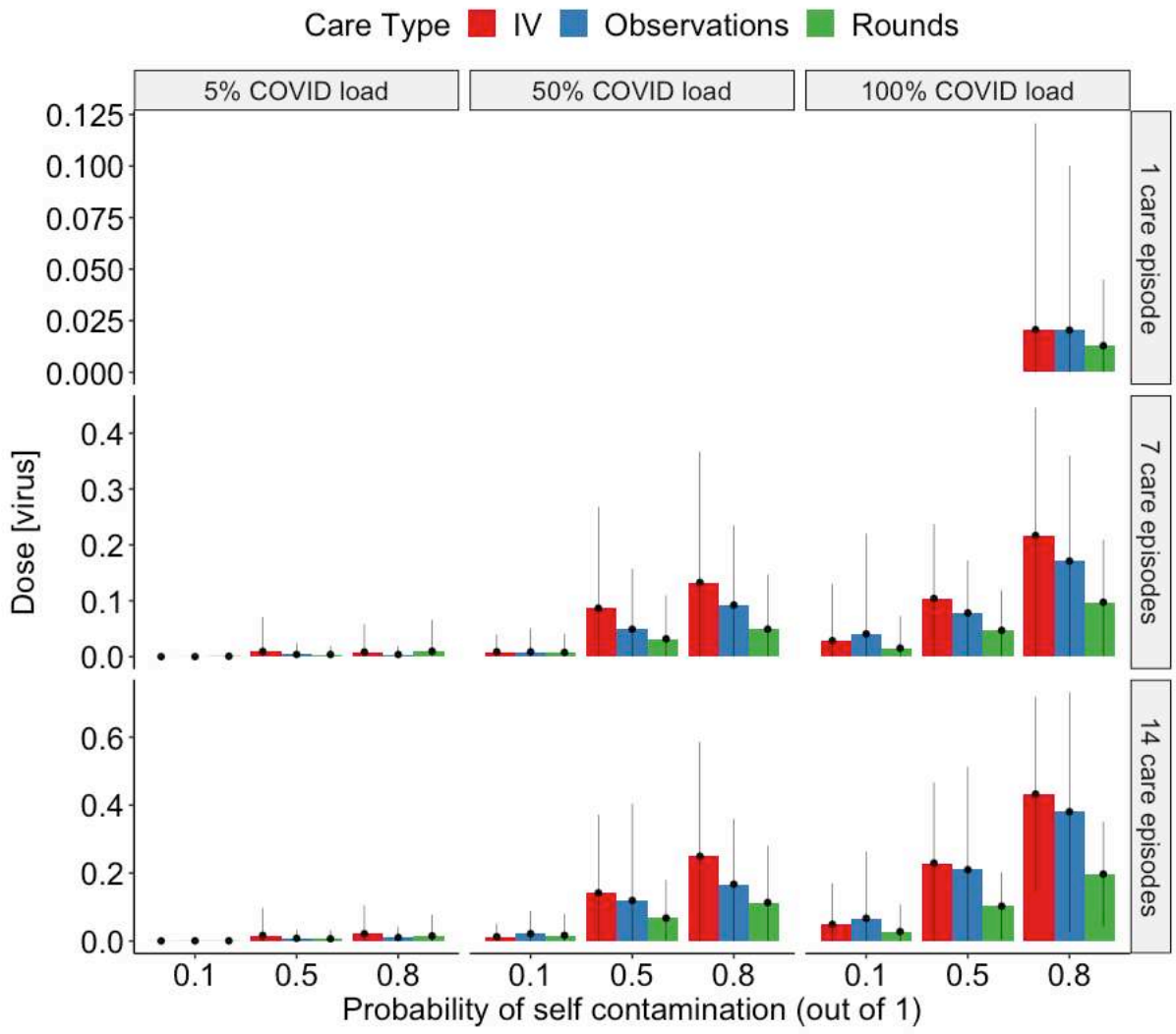

Figure 3: Bar chart showing viral dose (PFU) per shift for IV, Observations and doctors' rounds for different COVID patient loads. Errorbars represent standard deviation of the mean.

A linear regression of dose on all predictor variables conducted in R (version 4.0.1) shows that dose does not track linearly with COVID-19 prevalence ($p<0.001$); where the median dose received during 100% COVID-19 prevalence was an order of magnitude higher than at 50% (0.008 PFU vs 0.031PFU) and 0PFU after care with a ward of 5% COVID-19 patients.

Spearman correlation coefficients for input parameters vs viral dose received are given in Table2. In terms of most important factors determining exposure, surface cleanliness was found to be the single most important, with hand-to-mouth/eyes/nose transfer efficiency only half as important (correlation coefficient ρ = 0.29 vs ρ = 0.12, respectively) (see Table 3). Surface concentration relates to cleaning frequency and hence the control case was run for half the surface bioburden.

Table 3. Spearman correlation coefficients of input parameters with viral dose

Parameter	Spearman Correlation Coefficient
Concentration on surfaces (viral particles/cm^2)	0.27
Transfer efficiency to mouth, eyes, or nose**	0.08
Transfer efficiency surface to hand	0.03
Transfer efficiency Hand to surface	0.01
Inactivation constant for surfaces	-0.02
Fraction of total hand surface area in contact	-0.02
Fraction of RNA relating to infectious particles*	0.04
Fraction of total hand surface area used in hand-to-face contact**	0.03
Total hand surface area**	0.02
Inactivation constant for hands	0.02

*The spearman correlation coefficient represents instances where contacts with surfaces that had non-zero concentrations were made

**The spearman correlation coefficient represents instances in which these parameters were used in a simulation where a contaminated hand-to-face contact was made after doffing

410

Discussion

Key Findings and Generalizability

The model developed in this study indicates that exposure from mistakes after doffing PPE is likely to be low for a single shift, even for nurses on 100% patient COVID-19 positive wards. Exposure doses vary by care type as greater frequencies of surface contacts directly impact on viral loading on gloves and subsequent self-contamination exposures. The dose increases further if error rates in doffing are high and a high proportion of patients are COVID-19 positive (Figure 3) which highlights the importance of optimal hand hygiene, especially after PPE doffing.

Surface cleanliness was the most important factor in predicting dose regardless of doffing mistake likelihood, highlighting the relevance of frequency of cleaning regimes for managing risk. Halving the surface viral concentration decreased the exposure 2-fold. Studies have shown that microorganisms can be readily transferred between touch sites in a healthcare environment by routine activities(46). Dispersion of respiratory droplets and aerosols may contaminate less frequently touched surfaces as well, particularly where the patient is undergoing treatment that generates aerosols such as continuous positive airway (CPAP) ventilation. Sampling in COVID-19 wards suggests aerosol deposition is a contributor to surface contamination, as one study has reported deposition at a distance of 3m from the patient(11). Previous experimental work aerosolising a bacteria in an air-conditioned hospital room test-chamber showed that surfaces well outside the patient zone can become contaminated with infectious material (47, 48). Since the observational study underlying the Markov chains reveals that at least 10% of staff contacts impact on such surfaces (excluding door handles), then current lists of high-touch

surfaces(49) that had historically been prioritised for cleaning, may need to be revised.

A dose-response curve for SARS-CoV-2 is not yet available, and furthermore the contribution of each dose (i.e., upper respiratory vs lower respiratory route) to individual infection risk may still be unclear even if and when it is obtained (28). Consequently, we have analysed the results from the contact model based on relative exposures and qualitative trends to try and understand the effect of key parameters and mitigation strategies. In Figure 4 we plot the risk [0-1] for each of the doses that the nurses receive. We compare the prediction between the Beta Poisson dose-response curve presented above against that for HCoV229E. We also follow the approach from Lei et al. and assume that the dose required for infection from the upper respiratory tract relating to a mucosal contact is 100 times higher than a dose reaching the lower respiratory tract.

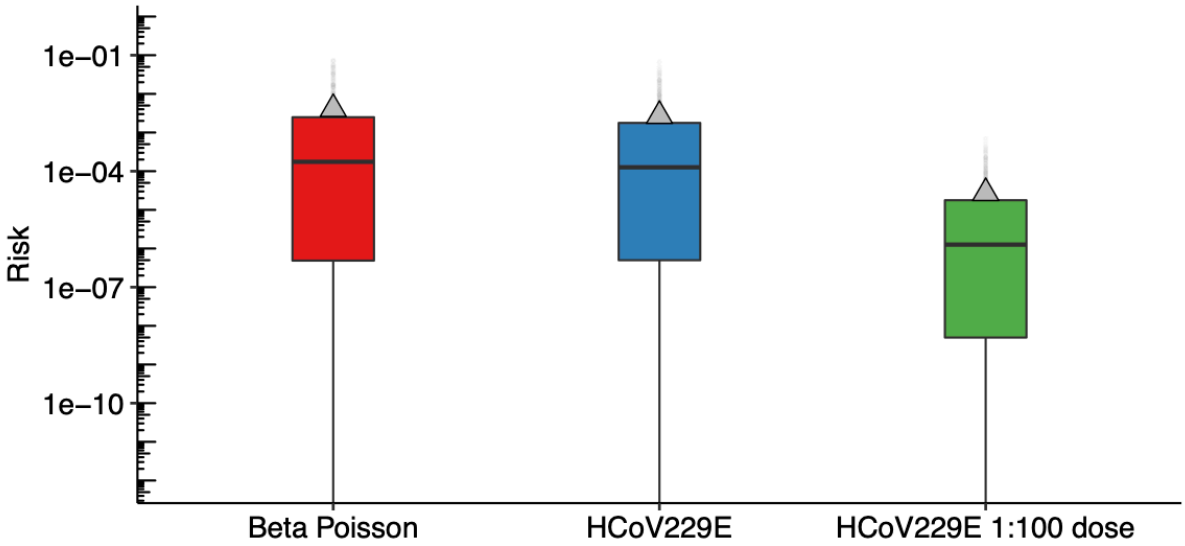

Figure 4 Boxplot showing Infection risk (i.e., individual probability of infection for each predicted dose), using the Beta-Poisson and HCoV-229E exponential dose-response curve (28). Triangles represent mean values.

452 In general, the mean risk is higher than the upper quartile alluding to the
453 hypothesis that a few nurses may become infected which relates to opportunistic or
454 rare events under these circumstances. Using a Bernoulli distribution with either a 1 or
455 a 0 response, representing an infection or not from each one of the predicted
456 exposure doses and corresponding individual infection risk probabilities, we can
457 predict the number of nurses infected per 100 nurses.
458 From the individual risks predicted using the Beta-Poisson curve and under a
459 baseline assumption of 5% COVID-19 positive patients, 14 care episodes, 10%
460 chance of self-inoculation we see that 1 nurse is likely to become infected with
461 another 1 possible based on the mean and standard deviations obtained from 100
462 Bernoulli simulation runs. Under the worst case scenario which could be roughly
463 interpreted as an out-of-control epidemic in the community (100% COVID-19
464 patients, 14 care episodes, 80% chance of self-inoculation), this mean increases to 4
465 per 100 with a standard deviation of 4 infections.
466 The results in Figure 4 are illustrative to demonstrate the potential variability in
467 infection risk that could result from exposures during a shift, but it is important to
468 recognise that, analysis of infection risk also needs to be interpreted in the context of
469 the current status of the pandemic within a particular country or region. Emergence
470 of more transmissible variants are already changing the exposure-risk relationships,
471 and it is likely that dose-response will be specific to a particular variant. The risk of
472 infection will also be substantially impacted by the vaccination status within a
473 community. At the time of writing, 45 million people had received the first vaccine
474 dose and 34 million the second dose in the UK, which will substantially reduce the
475 likelihood of infection further than those illustrated here.

476

477 Regardless of the number of COVID-19 positive patients on a ward, notable
478 decreases in predicted infection risk were associated with less self-contamination
479 during doffing. For example, for scenarios involving all COVID-19 patients, the mean
480 infection risk for 10% probability of self-contamination while doffing was 0.4%, while
481 the mean infection risk for an 80% probability of self-contamination while doffing was
482 more than a 420% increase at 2.1%. This emphasizes the importance of adequate
483 training for PPE use. Less risk of self-contamination will decrease transmission risks,
484 potentially through sanitizing gloves with alcohol gel before doffing. PPE can be an
485 effective strategy for mitigating exposure if proper doffing techniques are used. In
486 addition to training, improvements in PPE design that enhance safety and
487 expediency of doffing may lower self-contamination rates and therefore improve
488 PPE as a mitigation strategy (50). For example, fasteners or ties on gowns/masks were
489 identified as "doffing barriers," because it was unclear whether these were to be
490 untied and there were difficulties in reaching these ties. Self-contamination due to
491 gowns and masks were not specifically addressed in this model. It is possible that
492 self-contamination during doffing of items other than gloves could increase
493 potential risks due to incorrect doffing. Shortages of PPE have changed normal
494 practice where PPE is worn on a sessional basis rather than renewed for each
495 patient. This means less doffing and potentially less auto-contamination but may
496 increase the risk of virus transfer within the unit.

497 In addition to the importance of safe and proper doffing, the results from this
498 computational study also emphasize the importance of surface decontamination
499 and environmental monitoring strategies. The concentration of virus on surfaces was

500 the most influential parameter on dose, which is consistent with other surface
501 exposure studies (31). Whilst SARS-CoV-2 RNA has been detected on surfaces, one
502 limitation to a molecular approach is the lack of information regarding infectivity. In
503 a recent study by Zhou et al. (2020), no surface samples demonstrated infectivity.
504 However, it was noted that the concentrations of SARS-CoV-2 on surfaces were
505 below the current detection limits for culture methodologies (39). While there are
506 known relationships between cycle threshold values and probabilities of detecting
507 viable virus in a sample (12, 51), it is necessary to know what fraction of detected
508 genome copies relate to viral particles for QMRAs. More data are needed to better
509 understand how molecular concentrations, even concentrations below detection
510 limits, relate to infectivity and subsequent infection risk.

511 ***Model Uncertainties***

512 The model in this study only evaluates a surface transmission route while in
513 reality, risks posed to healthcare workers are due combined exposure pathways: air,
514 droplet, person-to-person, and surface transmission. As the model only evaluates
515 surface transmission, these infection risks are likely to be an underestimate of the
516 total risk incurred by healthcare workers over an entire shift. In a study of healthcare
517 workers in a facility in Wuhan, China, 1.1% (110/9684) were COVID-19 positive (52).
518 According to CDC, from February 12 – April 9, 2020, 19% (9,282/49,370) of COVID-19
519 U.S. cases for which healthcare professional status was available, were healthcare
520 workers (53). However, it is not known how many shifts were associated with these
521 infection rates. Additionally, we assumed that wards with non-COVID-19 patients did
522 not have SARS-CoV-2 contamination on surfaces, due to lack of data on SARS-CoV-
523 2 surface contamination beyond COVID-19 wards or patient rooms. There is

potential for asymptomatically infected healthcare workers to contribute environmental contamination, especially when considering the relatively long shedding durations for asymptomatic infections (54). Infected healthcare workers and environmental contamination could be considered in future extensions of this model.

The fact that the proportions of healthcare workers with COVID-19 discussed above are much larger than the infection risks estimated suggest that other transmission routes could drive additional HCW cases. This would include more transmission through airborne routes, or HCW to HCW transmission by asymptomatic cases outside the COVID-19 care environment (55). However, while there continues to be disagreement over the contribution of each route to overall risk, transmission routes influence each other, making them all significant in healthcare environments. For example, surfaces can become contaminated due to deposition of aerosolized virus. Viruses can later be resuspended from surfaces, contributing to air contamination. Future work should extend current models with a multi-exposure pathway approach. This will advance not only our understanding of SARS-CoV-2 transmission but the transmission of pathogens in built environments as a whole.

It should be noted that there is still a large variation in gowns and masks and that there is the possibility of double gloving, hence potentially reducing the risk of self-contamination and the type of material and the design will also to an extent, determine the contamination risk.

Finally, a dose-response curve informed by SARS-CoV-1 and HCoV-229E data was utilized, due to lack of SARS-CoV-2-specific dose-response data. Despite

549 limitations related to dose-response, the conclusions from the estimated doses were
550 consistent with insights from infection risk estimates. Increases in probability of
551 contamination between care episodes related to increases in dose and most
552 notably, for scenarios in which more than 5% of patients had COVID-19 (Figure 3).

553 *Conclusion*

554 We propose a model for predicting exposure to healthcare workers from self-
555 contamination during doffing of personal protective equipment over a single shift.
556 The model estimates the quantity of SARS-CoV-2 virus accretion on gloved hands for
557 three types of non-aerosol-generating procedures: IV-care, observations and
558 doctors' rounds. Once doffing was in progress, staff self-contaminated a fraction of
559 the times based on patient-load fatigue. Three COVID-19 positive patient scenarios
560 (5%, 50% and 100% COVID-19 patients) were investigated amounting to a total of
561 30,000 parameter combinations allowing us to conduct a "what-if" parametric study
562 and sensitivity analysis. Surface viral concentration was found to be more than twice
563 as important as any other factor whereby highlighting the importance of time-
564 appropriate cleaning. Transfer efficiency from finger to nose was of secondary
565 importance, although hand hygiene following doffing is still highly recommended.
566 Whilst exposure from this type of self-contamination is low per healthcare worker
567 shift, this highlights that the procedures, if carried out correctly, are generally safe. It
568 is accepted that other routes of transmission will play a significant role in infection
569 propagation.

570 *Conflicts of Interest*

571 None to declare

References

1. Johns Hopkins University. COVID-19 Dashboard by the Center for Systems Science and Engineering.
2. Boone SA, Gerba CP. 2007. Significance of fomites in the spread of respiratory and enteric viral disease. Appl Environ Microbiol 73:1687–1696.
3. Otter JA, Donskey C, Yezli S, Douthwaite S, Goldenberg SD, Weber DJ. 2016. Transmission of SARS and MERS coronaviruses and influenza virus in healthcare settings: The possible role of dry surface contamination. J Hosp Infect 92:235–250.
4. Kraay ANM, Hayashi MAL, Hernandez-Ceron N, Spicknall IH, Eisenberg MC, Meza R, Eisenberg JNS. 2018. Fomite-mediated transmission as a sufficient pathway: a comparative analysis across three viral pathogens. BMC Infect Dis 18:540.
5. Santarpia JL, Rivera DN, Herrera V, Morwitzer MJ, Creager H, Santarpia GW, Crown KK, Brett-Major D, Schnaubelt E, Broadhurst MJ, Lawler J V, Reid SP, Lowe JJ. 2020. Transmission Potential of SARS-CoV-2 in Viral Shedding Observed at the University of Nebraska Medical Center. medRxiv 2020.03.23.20039446.
6. Ye G, Lin H, Chen L, Wang S, Zeng Z, Wang W, Zhang S, Rebmann T, Li Y, Pan Z, Yang Z, Wang Y, Wang F, Qian Z, Wang X. 2020. Environmental contamination of the SARS-CoV-2 in healthcare premises: An urgent call for protection for healthcare workers. medRxiv 2020.03.11.20034546.
7. van Doremalen N, Bushmaker T, Morris DH, Holbrook MG, Gamble A, Williamson BN, Tamin A, Harcourt JL, Thornburg NJ, Gerber SI, Lloyd-Smith JO, de Wit E, Munster VJ. 2020. Aerosol and Surface Stability of SARS-CoV-2 as Compared with SARS-CoV-1. N Engl J Med.
8. Casanova LM, Erukunuakpor K, Kraft CS, Mumma JM, Durso FT, Ferguson AN, Gipson CL, Walsh VL, Zimring C, Dubose J, Jacob JT, Control D, Program PE. 2018. Assessing Viral Transfer During Doffing of Ebola-Level Personal Protective Equipment in a Biocontainment Unit. Clin Infect Dis 66:945–949.
9. Tomas ME, Kundrapu S, Thota P, Sunkesula VCK, Cadnum JL, Mana TSC, Jencson A, O'Donnell M, Zabarsky TF, Hecker MT, Ray AJ, Wilson BM, Donskey CJ. 2015. Contamination of health care personnel during removal of personal protective equipment. JAMA Intern Med 175:1904–1910.
10. Ong SWX, Tan YK, Chia PY, Lee TH, Ng OT, Wong MSY, Marimuthu K. 2020. Air, Surface Environmental, and Personal Protective Equipment Contamination by Severe Acute Respiratory Syndrome Coronavirus 2 (SARS-CoV-2) from a Symptomatic Patient. JAMA - J Am Med Assoc 323:1610–1612.
11. Liu Y, Ning Z, Chen Y, Guo M, Liu Y, Gali NK, Sun L, Duan Y, Cai J, Westerdahl D, Liu X, Xu K, Ho K fai, Kan H, Fu Q, Lan K. 2020. Aerodynamic analysis of SARS-CoV-2 in two Wuhan hospitals. Nature 582:557–560.
12. Bullard J, Dust K, Funk D, Strong JE, Alexander D, Garnett L, Boodman C, Bello A, Hedley A, Schiffman Z, Doan K, Bastien N, Li Y, Van Caeseele PG, Poliquin G. 2020. Predicting infectious SARS-CoV-2 from diagnostic samples. Clin Infect Dis 1–18.
13. WHO. 2016. Quantitative Microbial Risk Assessment: Application for Water Safety Management. WHO Press 187.

619 14. King MF, Noakes CJ, Sleigh PA. 2015. Modelling environmental contamination
620 in hospital single and four-bed rooms. Indoor Air 25:694–707.
621 15. King M-F, López-García M, Atedoghu KP, Zhang N, Wilson AM, Weterings M,
622 Hiwar W, Dancer SJ, Noakes CJ, Fletcher LA. 2020. Bacterial transfer To
623 fingertips during sequential surface contacts with and without gloves. Indoor
624 Air In print.
625 16. Wilson AM, Reynolds KA, Sexton JD, Canales RA. 2018. Modeling surface
626 disinfection needs to meet microbial risk reduction targets. Appl Environ
627 Microbiol 84:1–9.
628 17. Wilson AM, Reynolds KA, Jaykus LA, Escudero-Abarca B, Gerba CP. 2019.
629 Comparison of estimated norovirus infection risk reductions for a single fomite
630 contact scenario with residual and nonresidual hand sanitizers. Am J Infect
631 Control [in press].
632 18. Wilson AM, Reynolds KA, Canales RA. 2019. Estimating the effect of hand
633 hygiene compliance and surface cleaning timing on infection risk reductions
634 with a mathematical modeling approach. Am J Infect Control Article in Press.
635 19. Beamer PI, Plotkin KR, Gerba CP, Sifuentes LY, Koenig DW, Reynolds K a. 2015.
636 Modeling of human viruses on hands and risk of infection in an office
637 workplace using micro-activity data. J Occup Environ Hyg 12:266–75.
638 20. Guo Z-D, Wang Z-Y, Zhang S-F, Li X, Li L, Li C, Cui Y, Fu R-B, Dong Y-Z, Chi X-Y,
639 Zhang M-Y, Liu K, Cao C, Liu B, Zhang K, Gao Y-W, Lu B, Chen W. 2020. Aerosol
640 and Surface Distribution of Severe Acute Respiratory Syndrome Coronavirus 2
641 in Hospital Wards, Wuhan, China, 2020. Emerg Infect Dis 26.
642 21. Rusin P, Maxwell S, Gerba C. 2002. Comparative surface-to-hand and
643 fingertip-to-mouth transfer efficiency of gram-positive bacteria, gram-
644 negative bacteria, and phage. J Appl Microbiol 93:585–92.
645 22. Sizun J, Yu MWN, Talbot PJ. 2000. Survival of human coronaviruses 229E and
646 OC43 in suspension and after drying on surfaces : a possible source of hospital-
647 acquired infections. J Hosp Infect 46:55–60.
648 23. Kasloff SB, Strong JE, Funk D, Cutts T. 2020. Stability of SARS-CoV-2 on Critical
649 Personal Protective Equipment. medRxiv.
650 24. Kampf G, Todt D, Pfaender S, Steinmann E. 2020. Persistence of coronaviruses
651 on inanimate surfaces and its inactivation with biocidal agents. J Hosp Infect
652 104:246–251.
653 25. Girou E, Loyeau S, Legrand P, Oppein F, Brun-Buisson C. 2002. Efficacy of
654 handrubbing with alcohol based solution versus standard handwashing with
655 antiseptic soap: randomised clinical trial. BMJ 325:362–362.
656 26. AuYeung W, Canales RA, Leckie JO. 2008. The fraction of total hand surface
657 area involved in young children's outdoor hand-to-object contacts. Environ
658 Res 108:294–299.
659 27. U.S. Environmental Protection Agency. 2011. Exposure Factors Handbook 2011
660 Edition (EPA/600/R-09/052F). Washington, DC.
661 28. Watanabe T, Bartrand TA, Weir MH, Omura T, Haas CN. 2010. Development of
662 a dose-response model for SARS coronavirus. Risk Anal 30:1129–1138.
663 29. King M-F, Wilson AM, López-García M, Proctor J, Peckham DG, Clifton IJ,
664 Dancer SJ, Noakes CJ. 2020. Why is mock care not a good proxy for predicting
665 hand contamination during patient care? J Hosp Infect.
666 30. Jinadatha C, Villamaria FC, Coppin JD, Dale CR, Williams MD, Whitworth R,

667 Stibich M. 2017. Interaction of healthcare worker hands and portable medical
668 equipment: A sequence analysis to show potential transmission opportunities.
669 BMC Infect Dis 17:1–10.
670 31. Julian TR, Canales RA, Leckie JO, Boehm AB. 2009. A model of exposure to
671 rotavirus from nondietary ingestion iterated by simulated intermittent contacts.
672 Risk Anal 29:617–632.
673 32. King MF, Noakes CJ, Sleigh PA, Bale S, Waters L. 2016. Relationship between
674 healthcare worker surface contacts, care type and hand hygiene: An
675 observational study in a single-bed hospital ward. J Hosp Infect 94:48–51.
676 33. Harbourt DE, Haddow AD, Piper AE, Bloomfield H, Kearney BJ, Fetterer D,
677 Gibson K, Minogue T. 2020. Modeling the Stability of Severe Acute Respiratory
678 Syndrome Coronavirus 2 (SARS-CoV- 2) on Skin, Currency, and Clothing.
679 medRxiv.
680 34. Biryukov J, Boydston JA, Dunning RA, Yeager JJ, Wood S, Reese AL, Ferris A,
681 Miller D, Weaver W, Zeitouni NE, Phillips A, Freeburger D, Hooper I, Ratnesar-
682 Shumate S, Yolitz J, Krause M, Williams G, Dawson DG, Herzog A, Dabisch P,
683 Wahl V, Hevey MC, Altamura LA. 2020. Increasing Temperature and Relative
684 Humidity Accelerates Inactivation of SARS-CoV-2 on Surfaces. mSphere 5:1–9.
685 35. Pancic F, Carpentier DC, Came PE. 1980. Role of infectious secretions in the
686 transmission of rhinovirus. J Clin Microbiol 12:567–571.
687 36. Whiteley GS, Glasbey TO, Fahey PP. 2016. A suggested sampling algorithm for
688 use with ATP testing in cleanliness measurement. Infect Dis Heal 21:169–175.
689 37. Public Health England. 2017. Detection and enumeration of bacteria in swabs
690 and other environmental samples. Natl Infect Serv Food Water Environ
691 Microbiol Stand Method 4.
692 38. Margas E, Maguire E, Berland CR, Welander F, Holah JT. 2013. Assessment of
693 the environmental microbiological cross contamination following hand drying
694 with paper hand towels or an air blade dryer. J Appl Microbiol 115:572–582.
695 39. Zhou AJ, Otter JA, Price JR, Cimpeanu C, Garcia M, Kinross J, Boshier PR,
696 Mason S, Bolt F, Alison H, Barclay WS. 2020. Investigating SARS-CoV-2 surface
697 and air contamination in an acute healthcare setting during the peak of the
698 COVID-19 pandemic in London. medRxiv 1–24.
699 40. Van Abel N, Schoen ME, Kissel JC, Meschke JS. 2016. Comparison of Risk
700 Predicted by Multiple Norovirus Dose–Response Models and Implications for
701 Quantitative Microbial Risk Assessment. Risk Anal 37:245–264.
702 41. Beamer PI, Luik CE, Canales RA, Leckie JO. 2012. Quantified outdoor micro-
703 activity data for children aged 7 – 12-years old. J Expo Sci Environ Epidemiol
704 22:82–92.
705 42. Lopez GU, Gerba CP, Tamimi AH, Kitajima M, Maxwell SL, Rose JB. 2013.
706 Transfer efficiency of bacteria and viruses from porous and nonporous fomites
707 to fingers under different relative humidity conditions. Appl Environ Microbiol.
708 43. Xie G, Roiko A, Stratton H, Lemckert C, Dunn PK, Mengersen K. 2017. Guidelines
709 for use of the approximate beta-Poisson dose–response model. Risk Anal
710 37:1388–1402.
711 44. Canales RA, Wilson AM, Sinclair RG, Soto-Beltran M, Pearce-Walker J, Molina
712 M, Penny M, Reynolds KA. 2019. Microbial study of household hygiene
713 conditions and associated Listeria monocytogenes infection risks for Peruvian
714 women. Trop Med Int Heal 24:899–921.

45. Canales RA, Reynolds KA, Wilson AM, Fankem SLM, Weir MH, Rose JB, Ad-Elmaksoud S, Gerba CP. 2019. Modeling the role of fomites in a norovirus outbreak. J Occup Environ Hyg 16:16–26.
46. Rawlinson S, Ciric L, Cloutman-Green E. 2020. COVID-19 pandemic – let's not forget surfaces. J Hosp Infect 5–6.
47. King MF, Noakes CJ, Sleigh PA, Camargo-Valero MA. 2013. Bioaerosol deposition in single and two-bed hospital rooms: A numerical and experimental study. Build Environ 59:436–447.
48. King MF, Camargo-Valero MA, Matamoros-Veloza A, Sleigh PA, Noakes CJ. 2017. An effective surrogate tracer technique for S. aureus bioaerosols in a mechanically ventilated hospital room replica using dilute aqueous lithium chloride. Atmosphere (Basel) 8.
49. Huslage K, Rutala WA, Gergen MF, Ascp MT, Sickbert-bennett EE, Weber DJ. 2013. Microbial Assessment of High- , Medium- , and Low-Touch Hospital Room Surfaces and Low-Touch Hospital Room Surfaces 34:211–212.
50. Baloh J, Reisinger HS, Dukes K, Da Silva JP, Salehi HP, Ward M, Chasco EE, Pennathur PR, Herwaldt L. 2019. Healthcare Workers' Strategies for Doffing Personal Protective Equipment. Clin Infect Dis 69:S192–S198.
51. La Scola B, Le Bideau M, Andreani J, Hoang VT, Grimaldier C. 2020. Viral RNA load as determined by cell culture as a management tool for discharge of SARS-CoV-2 patients from infectious disease wards. Eur J Clin Microbiol Infect Dis 39:1059–1061.
52. Lai X, Wang M, Qin C, Tan L, Ran L, Chen D, Zhang H, Shang K, Xia C, Wang S, Xu S, Wang W. 2020. Coronavirus Disease 2019 (COVID-2019) Infection Among Health Care Workers and Implications for Prevention Measures in a Tertiary Hospital in Wuhan, China. JAMA Netw open 3:e209666.
53. Hughes MM, Groenewold MR, Lessem SE, Xu K, Ussery EN, Wiegand RE, Qin X, Do T, Thomas D, Tsai S, Davidson A, Latash J, Eckel S, Collins J, Ojo M, McHugh L, Li W, Chen J, Chan J, Wortham jonathan M, Reagan-Steiner S, Lee JT, Reddy SC, Kuhar DT, Burrer SL, Stuckey MJ. 2020. Update: Characteristics of Health Care Personnel with COVID-19 — United States, February 12–July 16, 2020. Morb Mortal Wkly Rep 69.
54. Long Q-X, Tang X-J, Shi Q-L, Li Q, Deng H-J, Yuan J, Hu J-L, Xu W, Zhang Y, Lv F-J, Su K, Zhang F, Gong J, Wu B, Liu X-M, Li J-J, Qiu J-F, Chen J, Huang A-L. 2020. Clinical and immunological assessment of asymptomatic SARS-CoV-2 infections. Nat Med 1–5.
55. Sikkema RS, Pas SD, Nieuwenhuijse DF, Toole ÁO, Verweij J, Linden A Van Der, Chestakova I, Schapendonk C, Koopmans MPG. 2020. Articles COVID-19 in health-care workers in three hospitals in the south of the Netherlands : a cross-sectional study 3099:1–8.

Tables:

Table 1. Model parameters and their distributions/point values

Parameter	Distribution/Point Value	Reference
Surface contamination (C_{RNA}) (RNA/ swabbed surface area)	For infected patient scenarios Surfaces: Triangular (min=3.3 x 10^3, mid=2.8 x 10^4, max=6.6 x 10^4)	(20)

	Patient: Point estimate: 3.3 x 10^3	
Area of any given surface($A_{surface}$) (cm^2)	Triangular (min=5, max=195, mid=100)	Assumed
Fraction of RNA(*infective*) assumed to be infectious	Uniform (min=0.001, max=0.1)	Assumed
Finger-to-surface transfer efficiency (β) (fraction)	Normal (mean=0.118, sd=0.088) Left- and right-truncated at 0 and 1, respectively	(4)
Surface-to-finger transfer efficiency (λ) (fraction)	Normal (mean=0.123, sd=0.068) Left- and right-truncated at 0 and 1, respectively	(4)
Finger-to-mouth transfer efficiency ($TE_{H®M}$) (fraction)	Normal (mean=0.339, sd=0.1318) Left- and right-truncated at 0 and 1, respectively	(21)
Glove doffing self-contamination transfer efficiency	Uniform (min=3 x 10^{-7}, max=0.1)	(8)
T_{99} on Hands (hours) used for calculating inactivation constants	Uniform (min=1, max=8)	(22, 23)
T_{50} on surfaces (hours) used for calculating inactivation constants	Uniform (min=4.59, max=8.17)	(7)
Hand hygiene efficacy: alcohol gel (log_{10} reduction)	Uniform (min=2, max=4)	(24)
Hand hygiene efficacy: soap and water (log_{10} reduction)	Normal (mean=1.62, sd=0.12) Left-and right-truncated at 0 and 4, respectively	(25)
Fraction of total hand surface area for hand-to-mouth or hand-to-surface contacts ($S_m$and S_h)	For in/out events: Uniform (min=0.10, max=0.17) For patient contacts: Uniform (min=0.04, max=0.25) For other surface contacts: Uniform (min=0.008, max=0.25) For hand-to-face contacts: Uniform (min=0.008, max=0.012)	(26)
Total hand surface area (A_h) (cm^2)	Uniform (min=445, max=535)	(19, 27)
Dose response curve parameter* α	0.36 ± 0.25 0.12, 19.6	(28); This study
Dose response curve parameter* β	5.94 ± 11.4 0.27, 802.1	(28); This study

757

*Dose response curve parameters are to be used in bootstrapped pairs. Mean ± SD and minimum and maximum are provided to offer context as to the magnitude of these parameters.

763 **Table 2 PFU doses to for each care type**

QUANTILE	IV CARE	OBSERVATIONS	DRS ROUNDS
0%	0	0	0
25%	0	0	0
50%	0.00184	0.0021	0.00127
75%	0.0751	0.0651	0.0409
95%	0.506	0.421	0.234

764

765

766

767 **Table 3.** Spearman correlation coefficients of input parameters with infection risk

Parameter	Spearman Correlation Coefficient
Concentration on surfaces (viral particles/cm^2)	0.27
Transfer efficiency to mouth, eyes, or nose**	0.08
Transfer efficiency surface to hand	0.03
Transfer efficiency Hand to surface	0.01
Inactivation constant for surfaces	-0.02
Fraction of total hand surface area in contact	-0.02
Fraction of RNA relating to infectious particles*	0.04
Fraction of total hand surface area used in hand-to-face contact**	0.03
Total hand surface area**	0.02
Inactivation constant for hands	0.02

768
769 *The spearman correlation coefficient represents instances where contacts with
770 surfaces that had non-zero concentrations were made
771 **The spearman correlation coefficient represents instances in which these
772 parameters were used in a simulation where a contaminated hand-to-face contact
773 was made after doffing
774
775

776

777

778

Figure captions

Figure 5 Dose-response risk curve for averaged SARS CoV-1 and Coronavirus 229E response.

Figure 6 Stair plot of example HCW surface contacts during care, where "patient" is a hand-to-patient contact; "out" and "in" are exit and entrance into the patient room, respectively; "FarPatient" is a hand-to-far patient surface contact; and "Equipment" is a hand-to-equipment surface contact.

Figure 7: Bar chart showing dose per shift for IV, Observations and doctors' rounds for different COVID patient loads. Errorbars represent standard deviation of the mean.

Figure 8 Boxplot showing Infection risk (i.e., individual probability of infection for each predicted dose), using the Beta-Poisson and HCoV-229E exponential dose-response curve (28). Triangles represent mean values.

793

794

795
796

797